

Single-Crystal Vibrational Spectrum of Phenakite, Be_2SiO_4 , and Its Interpretation Using a Transferable Empirical Force Field

Tullio Pilati

*Centro CNR per lo Studio delle Relazioni tra Struttura e Reattività Chimica, Via Golgi 19,
I-20133 Milano, Italy*

Carlo Maria Gramaccioli* and Federico Pezzotta

*Dipartimento di Scienze della Terra, sez. Mineralogia, Università degli Studi, Via Botticelli 23,
I-20133 Milano, Italy*

Paola Fermo and Silvia Bruni

*Dipartimento di Chimica Inorganica, Metallorganica e Analitica, Università degli Studi, Via Venezian 21,
I-20133 Milano, Italy*

Received: November 5, 1997; In Final Form: March 13, 1998

Using an oriented single crystal, Raman and infrared vibrational spectra have been measured for phenakite, Be_2SiO_4 . The results have been interpreted on the grounds of Born–von Karman rigid-ion lattice-dynamical calculations, using empirical potentials derived from fitting the vibrational frequencies of a group of silicates, carbonates, and oxides, not including the substance under study. The very good agreement of our calculations with experimental data of independent origin and nature confirms the transferability of empirical potentials, and also their advantageous use for interpreting and reproducing the vibrational spectra of silicates and oxides in general.

1. Introduction

In recent years the study of vibrational spectra of solids obtained from single crystals has provided the possibility of comparing a notable number of experimentally observed frequencies with the corresponding calculated estimates obtained using models and routines of various theoretical complexity. Whenever such models prove to be reliable in terms of reproducing the values of the observed frequencies with good approximation, then a reasonable interpretation of the nature of each vibrational mode can also be expected. Moreover, such a procedure can often be quite useful in confirming the interpretation of the observed spectra, by distinguishing the true fundamentals from combinations, overtones, and also from spurious peaks that are often encountered experimentally.

Although, as for molecules, there has been a growing interest in developing “ab initio” quantum-mechanical calculations to reproduce the vibrational spectra of a number of crystals,¹ nevertheless, such calculations in practice are still restricted only to the simplest structures, and the routines become impracticable even for cases of moderate complexity. Therefore, at least in most instances, the best possibility at present for interpreting vibrational spectra in molecular or ionic crystals is that of using empirical potentials (especially if transferable) and Born–von Karman lattice-dynamical calculations of various degrees of sophistication (rigid ion, shell models, etc.).

Following our interest in the field, which started from molecular crystals,² we have tried to extend our Born–von

Karman harmonic lattice-dynamical calculations to minerals, initially considering some oxides such as corundum ($\alpha\text{-Al}_2\text{O}_3$), quartz ($\alpha\text{-SiO}_2$), coesite (SiO_2), chrysoberyl (Al_2BeO_4), and bromellite (BeO) and then also silicates such as the olivine group, garnets, andalusite (Al_2OSiO_4), kyanite (Al_2OSiO_4), diopside ($\text{CaMgSi}_2\text{O}_6$), beryl ($\text{Be}_3\text{Al}_2\text{Si}_6\text{O}_{18}$) and some carbonates such as calcite and aragonite (α - and β - CaCO_3), magnesite (MgCO_3), and dolomite [$\text{CaMg}(\text{CO}_3)_2$].^{2–13} In all these cases, our calculations were extended to the whole Brillouin zone; for the sake of simplicity, a rigid-ion (or rigid-atom) model was used. In this model, the electron cloud of each ion (or atom, in general) is assumed not to be deformed (or displaced from the nucleus) during motion.

The initial scope of our calculations was mostly connected with theoretical evaluation of atomic displacement parameters (ADPs), to compare their estimates with the corresponding results obtained from crystal-structure refinement; then, in view of their greater importance for materials science and petrology in general, we have increased our attention to interpreting vibrational spectroscopy data, such as Raman- and infrared spectra, to interpreting phonon dispersion curves, and especially to estimating the values of thermodynamic functions.

In agreement with other authors,^{14,15} our results indicate that even for ionic inorganic compounds, such as most minerals, the force fields are essentially transferable. For instance, we have shown^{8,9,12} that for grossular ($\text{Ca}_3\text{Al}_2\text{Si}_3\text{O}_{12}$), diopside, and coesite a force field optimized considering a series of different minerals not including the substance under study could predict the Raman and infrared spectra in detail, as well as the values of the specific heat and of entropy in a whole range of different temperatures.

* To whom correspondence should be addressed. E-mail: carlo@r10.terra.unimi.it.

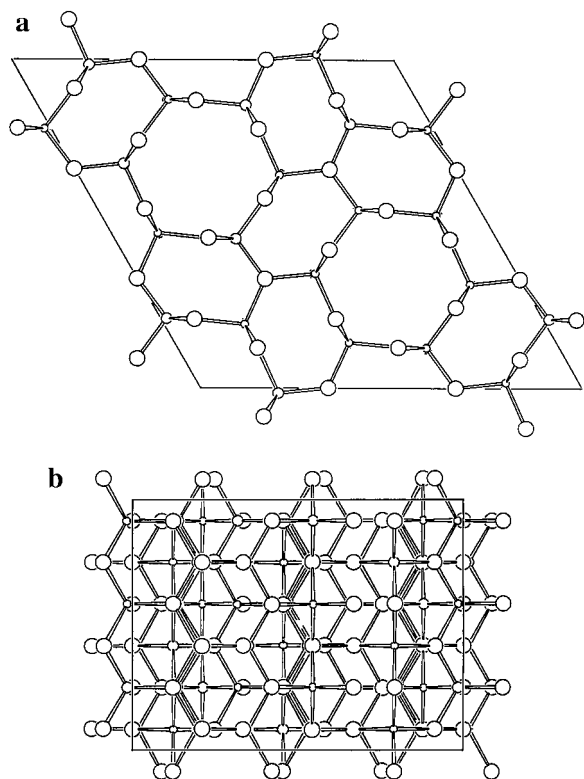


Figure 1. 1: Crystal structure of phenakite:²¹ (a) as seen along the crystallographic z axis; (b) as seen along the crystallographic y axis. The largest spheres are oxygen atoms, the smallest are beryllium atoms, and the intermediate ones are silicon atoms.

Our interest toward phenakite (Be_2SiO_4) in particular has developed because its structure is a relatively simple example of a complex problem. Although this substance has been long considered as a “nesosilicate”, i.e., as a substance with isolated SiO_4 tetrahedra, nevertheless such tetrahedra are joined together by strong BeO_4 tetrahedra to form a three-dimensional network or “giant molecule” structure including Be, Si, and O atoms, similar to quartz or to many of the so-called “tectosilicates” (see Figure 1). For this reason, phenakite is sometimes considered as a real tectosilicate, and some of its physical properties are similar to those of quartz (whence its name from a Greek term meaning “a deceiver”, since it resembles quartz).

In this case, and even more than for other silicates, a simple interpretation of the vibrational spectra derived from the fundamental modes of isolated tetrahedra as separate units (ν_1 to ν_4) is invalid, owing to the possibility of strong coupling, and in the crystal structure there are not even well-defined clusters of tetrahedra such as there are instead in ring- or chain silicates. For these reasons it is unrealistic to subdivide the vibrational modes of a phenakite crystal into “internal” and “external” modes with respect to the tetrahedral groups (SiO_4 or BeO_4) or clusters of such units, and even less justified is proceeding to further division of the latter modes into “translational” and “rotational” lattice modes, etc. Similarly, for these reasons, here it is not advisable to start lattice-dynamical calculations by considering first an isolated group of atoms and then taking the perturbation due to the crystal lattice into account (as was done instead for some other silicates^{16–18}); on the contrary, a lattice-dynamical interpretation of the modes *extended to the whole crystal* is needed from the beginning. Due to such difficulties, the success of these calculations in reproducing the vibrational spectra and in showing the existence of strong coupling between the tetrahedra of the whole structure (see below) is important in indicating to what extent such models

and computing routines represent a definite improvement with respect to earlier procedures, and this possibility of testing has been one of the main reasons why this particular substance has been considered.

2. Procedure of Calculation

Our calculations, as we have seen, proceed according to the “classic” rigid-ion lattice-dynamical model.^{3,8,19,20} Following a well-established scheme, from the second derivatives of the potential energy with respect to the positional coordinates of all the atoms in the primitive unit cell the dynamical matrix is built. The square roots of the eigenvalues of this matrix (mass-weighted) correspond to the vibrational frequencies of the various normal modes, whereas the components of the eigenvectors characterize the shift and the phase of each particular atom in the normal modes.

For these calculations, we used a program entirely written by us; our routines include a number of new methods, involving, e.g., the evaluation of Coulombic lattice sums.¹⁹ The program input essentially consists of experimental crystallographic data (unit cell parameters and atomic fractional coordinates, symmetry space-group operations) and energy-determining information such as the atomic charge, type of valence force-field (VFF) empirical potential, and its parameters. A further possibility is also that of “refining” the empirical potentials, so that the best fit to some particular experimental data (such as, for instance, the vibrational frequencies of a group of substances) is obtained.

3. Experimental Section

Raman spectra were measured at room temperature using a JASCO TRS-300 Raman spectrometer and the 488 nm excitation line from an argon ion laser: the relative data were collected using a scattering geometry of both 90 and 180°. Infrared spectra were acquired using a BIO-RAD FTS-40 Fourier transform infrared spectrophotometer equipped with a SPECAC specular reflectance accessory (incidence angle = 12.5°). The reflection infrared data were processed using the Kramers–Kronig analysis. The sample of phenakite used here is a single gemmy crystal from the Malagasy Republic (Anjanabonoina, Betafo area) measuring about $1.2 \times 0.8 \times 0.8$ cm, accurately cut and polished on the faces (100) and (001). On consideration of the crystal structure of phenakite, which is represented in Figure 1 (space group C_{3i}^2 , with all atoms on general positions, and with 6 formula units Be_2SiO_4 per primitive cell or 18 per R-centered nonprimitive cell²¹), and application of the standard group theoretical analysis, 21 E_g modes and 21 A_g modes (both Raman active), as well as 20 E_u modes and 20 A_u modes (both infrared active), are expected. In agreement with theory, 21 E_g modes were detected by our instrument (however, the lowest one is spurious: see below); of the 21 expected A_g modes 16 only were observed (see also Figure 2). With respect to earlier investigations reported in the literature, our Raman data are the first measurements ever performed on a single crystal, and for which the symmetry labeling is certain. It is worth remembering that for a crystal whose point group symmetry is C_{3i} the A_g modes correspond to nonzero xx , yy , and zz components of the scattering tensor; for the E_g modes, the xx , yy , xy , xz , and yz components are different from zero.²² Therefore, only the spectra obtained with (zz) , (yx) , (zx) , and (yz) polarization of the incident and scattered radiation, respectively, show bands that can be assigned to modes of a single-symmetry species; furthermore, for the (xz) - and (yz) -polarized spectra, the bands are expected to have the same relative intensity, and such a situation was indeed confirmed experimentally. Since the (zz) -, (yx) -, and (zx) -polarized Raman spectra are the most meaningful

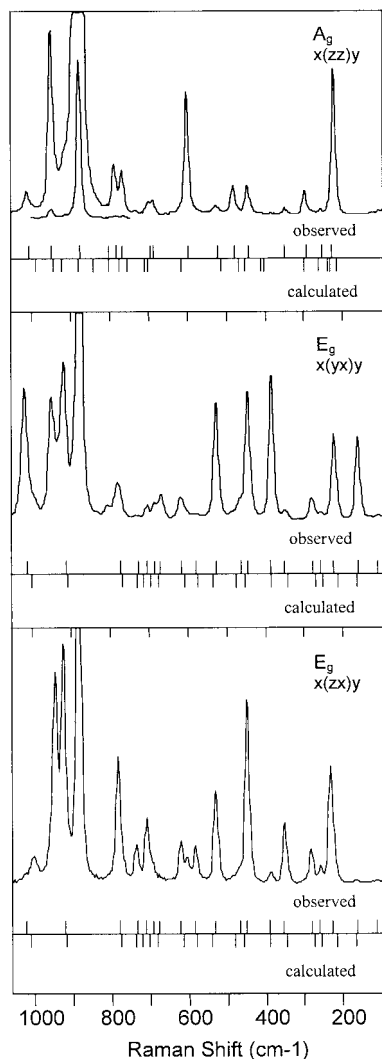


Figure 2. Polarized Raman spectra of phenakite. The polarization of light and the orientation of the crystal are labeled $\alpha(\beta\gamma)\delta$, where α and δ indicate the directions of propagation and β and γ the directions of polarization of the incident and the scattered radiation, respectively. The choice of the Cartesian reference axes x , y , and z was made according to ref 27, assuming z to be parallel to the 3-fold symmetry axis of the crystal. The intensities are given in arbitrary units.

ones, such data only are shown in the figures. It should be noted that, due to its strong intensity, a residue of the A_g band at 878 cm^{-1} is always present, even in the (yx) - and (zx) -polarized spectra, where the presence should be limited to the E_g modes only. The close agreement between our single-crystal data and the corresponding Raman powder spectrum²³ has permitted us to assign a reasonable symmetry labeling to the latter (see Table 1).

Of the 20 expected infrared active E_u modes, and of the 20 A_u modes, 13 and 19 were measured by us, respectively [the IR activity is $A_u(z)$, and $E_u(x,y)$] (see also Figure 3); however, according to our interpretation, at least two and four of them, respectively, are not true fundamentals (see below). There is good agreement with the values obtained from a single crystal at room temperature,²⁴ with the exception of some TO-LO splittings observed for a few high-frequency modes; however, our data seem to agree better with theoretical calculations (see below). On the whole, all the frequencies observed earlier²³ were also measured by us. Several additional modes are found in our data, indicating our set of observations to be more complete.

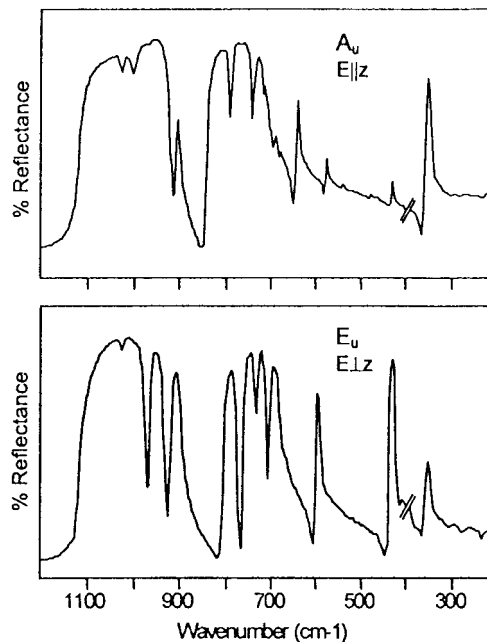


Figure 3. Polarized infrared spectra of phenakite. Full scale indicates 100% reflectance.

Even more markedly than for the Raman-active modes, most of the missing infrared data seem to be at the lowest frequencies, since none in fact were noticed below 340 cm^{-1} in the spectrum taken from a single crystal. According to our calculations (see below) in the $200\text{--}340\text{ cm}^{-1}$ range three additional E_u frequencies, and four A_u frequencies should also be observed. The existence of such low-frequency modes is also shown in the powder data,²³ which are in good agreement with some of our own calculated mode frequencies.

4. Results and Discussion

Assuming the charge to be the same for all the atoms of the same element (in the lack of more detailed criteria), with the exception of oxygen, whose charge is derived from the overall balance for each structure, all parameters of the force field used here (including the atomic charge) and reported in Table 2 have been obtained on a best-fit basis to vibrational frequencies. The force field includes Morse-type functions for stretching or oxygen–oxygen interaction, plus three-body (or four-body) interactions described as bond bending, bending–stretching, bending–bending, or stretching–stretching, respectively, most of which depend on the value of the angle.

The experimental data considered in the fit are mainly Raman and infrared spectra of a selected group of minerals, *not including phenakite*. This group includes silicates, such as forsterite (Mg_2SiO_4), monticellite (CaMgSiO_4), andalusite (Al_2OSiO_4), diopside ($\text{CaMgSi}_2\text{O}_6$), and beryl ($\text{Be}_3\text{Al}_2\text{Si}_6\text{O}_{18}$), oxides such as quartz ($\alpha\text{-SiO}_2$), corundum ($\alpha\text{-Al}_2\text{O}_3$), bromellite (BeO), and chrysoberyl (Al_2BeO_4), and carbonates, such as calcite ($\alpha\text{-CaCO}_3$), aragonite ($\beta\text{-CaCO}_3$), dolomite [$\text{CaMg}(\text{CO}_3)_2$], and magnesite (MgCO_3). Besides these spectra, the lowest branches of the phonon dispersion curves of quartz, forsterite, andalusite, and calcite were also considered. In deriving all these potentials, a weight inversely proportional to the square of the frequency was assigned to each observation.

In some papers dealing with lattice dynamics of silicates^{17,18} satisfactory results were obtained by using simpler empirical “short-range” force fields fitted to the specific substance to be studied. These fields include “stretching” metal–oxygen or silicon–oxygen constants together with O–Si–O bending

TABLE 1: Vibrational Frequencies (cm⁻¹) at Room Temperature^a

	obs(1)	obs(2)	cal		obs(1)	obs(2)	cal	
E _g	115			E _g	619	618	614	
	168	162	174		672	669	675	
	236	222	225		686	689	707	
	262	257	257		705	705	720	
	285		277		731	730	734	
	355	350	347		778		774	
	389	389	388				846	
	449	447	457		918	916	920	
	470	466	496		929	924	926	
	528	527	539		992	999	970	
	580	578	577		1018	1020	999	
	A _g				213	A _g	689	
236		233	245	700			723	
		257	248	768	768		730	
261		283	272	787	788		748	
302			310	805	807		805	
353		350	416				853	
			424	878	877		881	
449		447	460				918	
486		483	468	949	952		943	
528		527	505	1011			956	
603			640					
E _u (TO-LO)				235–235	E _u (TO-LO)		686–702	683–808
		(294.1)	284–284	689–		706–716		
		(304.7)	308–308	709–731		710–704	721–733	
	355–359	357–358	353–353	733–760		734–733	744–778	
		(384.5)	380–381	775–806		778–768	779–798	
	420–434	420–435	440–445				814–831	
	443–444		455–471	896–919		893–1110	891–899	
			529–530				923–935	
			567–569	933–966		931–917	941–973	
	592–600	590–600	598–600	972–1024		970–965	975–1077	
	669–			1024–1114		1019–		
	A _u (TO-LO)			234–234		A _u (TO-LO)	675–679	
			260–260					
		(294.1)	273–273	688–690			696–696	
		(316.5)	308–309	707–713	711–840		710–712	
347–358		348–361	365–385	715–736	719–			
428–		429–431	408–410		723–			
474–476			493–494	740–767	741–739		728–744	
541–544		544–545	525–526	763–786			754–820	
576–579		577–579	579–580	788–	792–791		820–837	
599–603				899–908	898–908		918–925	
636–644		636–643	639–639	921–968	922–1104		928–963	
665–667			649–649	970–999	964–964		964–983	
			999–1026	997–997	983–1073			

^a The calculated values correspond to the force field reported in Table 1. ^b obs(1): our data. obs(2): previous experimental data taken from the literature.^{23–24} For this second set of observations, the E_g and A_g frequencies are powder data, which have been tentatively labeled by us by comparison with the corresponding single-crystal data. Values within parentheses are from powder IR measurements.²³

constants, with no explicit involvement of atomic charges or of a specific O–O nonbonding interaction. In our case, instead, owing to inclusion of different series of compounds in the fitting procedure, thereby exploring a significant range of O–O contacts, and to the consequent superabundance of experimental data, our potentials include separate contributions of O–O nonbonding interaction, and also of bond-angle bending constants, together with Coulombic interaction. Such a more complex field has purposely been derived for extensive application to a number of different substances.

The calculated Raman- and infrared-active frequencies are reported in Table 1 for these potentials, together with the corresponding experimental results, either obtained by us or taken from the literature. The agreement is very good. Therefore, the possibility of carrying on these lattice-dynamical calculations successfully, using empirical potentials compatible with a wide group of different substances, is confirmed. In particular, the success in interpreting the vibrational spectrum

of phenakite starting from empirical potentials exclusively derived by fitting the experimental data relative to other compounds proves the satisfactory transferability of empirical potentials, in agreement with the results already published by us^{8,9,12} and other authors.^{14,15,25}

In view of the satisfactory agreement of our model with the available spectral data, the interpretation of the normal modes in the crystal is reasonably grounded. The components of the eigenvectors relative to the atoms in the asymmetric unit of the crystal and to the two highest frequencies are reported in Table 3: here it is clear that even for the high-frequency limit the motion of Be and the neighboring Si atoms is strongly correlated, thereby implying the existence of notable coupling between the atoms in different tetrahedra (SiO₄ or BeO₄ groups); another aspect of the same situation is shown in Figure 4, where a few significant vibrational modes as examples are represented.

As we expected (see above), this situation excludes the possibility of reasonable distinction between “internal” and

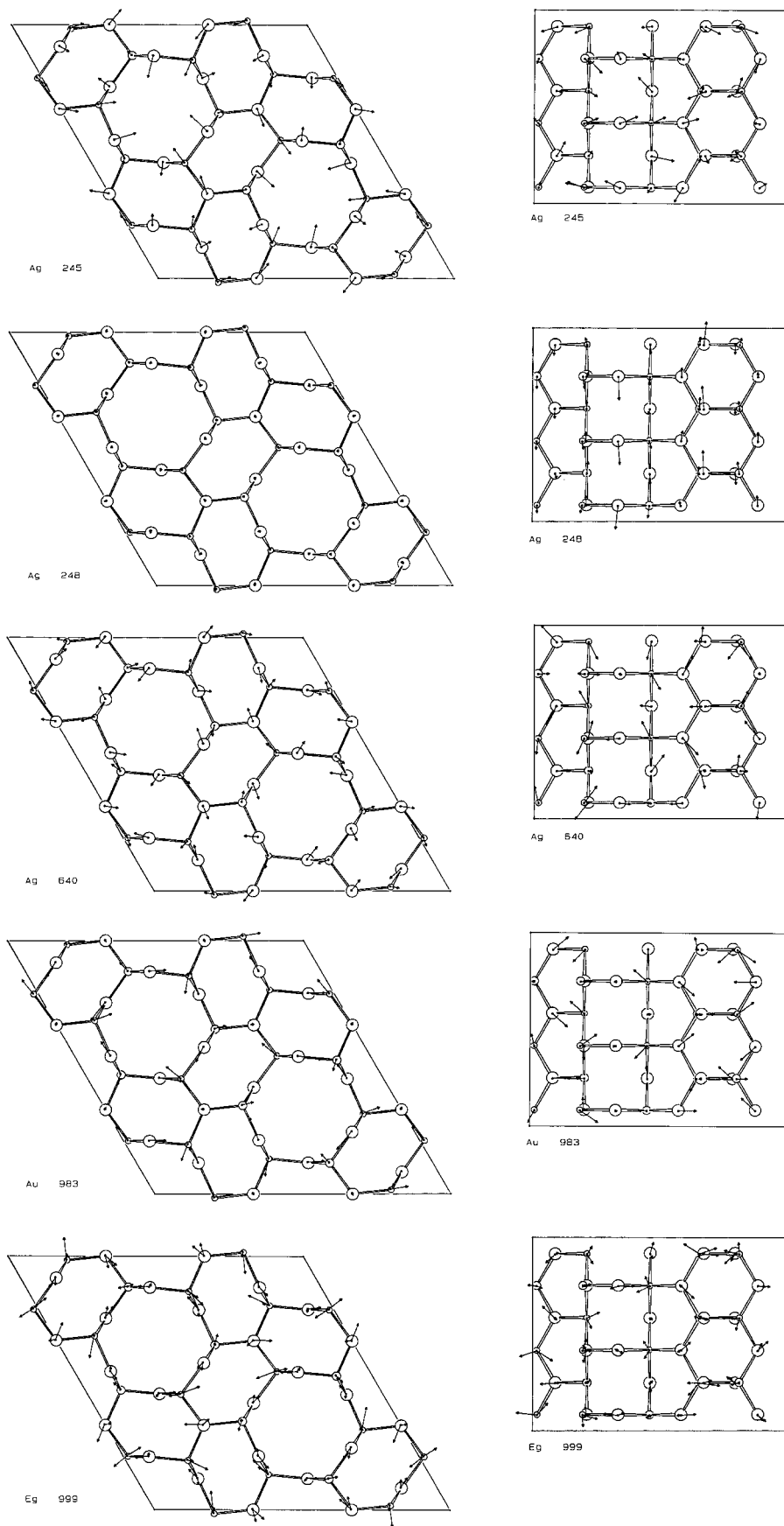


Figure 4. Calculated atomic motions for some normal modes in phenakite. The diagrams in the boxes to the left and right are the z axis and the y axis projections, respectively, and the structural details correspond to Figures 1a,b, respectively. Arrows (drawn to scale) indicate the relative amplitude of the motion of each atom in the normal mode. Owing to the complexity of the structure, which causes considerable overlapping, for clarity in the projections along the z axis only the atoms with z ranging from 0.31 to 0.69 (in unit cell fractions) are represented; similarly, for the projections along the y axis, only the atoms with y ranging from -0.03 – 0.28 (in unit cell fractions) are represented; here z is vertical.

TABLE 2: Empirical Potentials Used Here^a

Atomic Charge (electrons)			
Si	Be	O	
1.428 83	-1.172 92	by charge balance	
Stretching Potentials: Energy (kJ/mol) = $A\{\exp[-2B(r - C)] - 2 \exp[-B(r - C)]\}$			
	A	B	C
Si-O	2374.93	0.796 568	1.650 90
Be-O	5922.84	0.323 220	1.685 60
O-O (<5.5 Å)	15.0851	1.269 63	2.965 48
Bending Potentials for the Bond Angle β : $K [(\text{mdyn}\cdot\text{Å})/\text{rad}^2] =$ $A + B \cos \beta + C \cos^2 \beta$			
	A	B	C
O-Si-O	-0.052 092 7	-1.057 43	0.246 327
O-Be-O	0.023 535 2	-0.127 977	-0.444 620
Si-O-Si	0.260 788		
Be-O-Be	0.101 539		
Si-O-Be	-0.025 058 7		
Bending-Stretching: $K (\text{mdyn}\cdot\text{rad}) =$ $A + B (\beta - 109.47) (\beta \text{ in deg})$			
	A	B	
O-Si-O/Si-O	0.087 423 8	-0.441 941	
O-Be-O/Be-O	0.039 761 5	-0.005 319	
Stretching-Stretching (mdyn/Å)			
	A	B	
Si-O/Si-O		-0.039 659 4	
Be-O/Be-O		-0.056 083 7	

^a For Coulombic interactions, the reciprocal lattice was sampled up to $d^* = 1.7 \text{ \AA}^{-1}$.

TABLE 3: Components of Some Eigenvectors of the Three Highest Frequency Modes (Frequencies in cm^{-1} ; Polarization Vectors for the Atoms in the Asymmetric Unit $\times 1000$, Referred, in Sequence, to a Set of Cartesian Axes Parallel to a^* , b , c)^a

atom	A_u 983			E_g 999					
Si	129	-38	1	-92	-69	-5	-93	-97	-37
Be(1)	108	-41	80	-31	-95	79	-82	-168	-71
Be(2)	118	-21	-79	-87	-115	-56	-109	-112	98
O(1)	31	199	1	-3	194	11	46	-72	-7
O(2)	-20	10	0	205	-68	23	-52	94	27
O(3)	-120	-80	110	-32	26	12	112	74	-105
O(4)	-127	-74	-114	-58	7	-26	120	106	146

^a The asymmetric unit corresponds to that reported by Downs & Gibbs.²¹

“external” modes with respect to these tetrahedral groups, or also to definite clusters of such groups. Therefore, here each normal mode does imply an extensive deformation in the crystal, which can hardly be interpreted as a bending, stretching, or “lattice” mode only in the tetrahedral units, as it is too often found in the literature. Such earlier interpretations were originally taken from molecules; and there is still considerable reluctance in accepting a “lattice-dynamical” point of view relative to the whole crystal, even in cases (as here) where a single “molecular” group or cluster does not exist, all atoms and their coordination polyhedra being strictly connected with each other. A conclusion similar to ours has been drawn by other authors, when studying other silicates.^{16,26}

On considering the observed spectral data in some detail, our calculations agree very well with our spectral data, and the few cases showing some disagreement are very probably due to some kind of interference. For instance, the lowest observed E_g frequency at 115 cm^{-1} seems to differ too much from any theoretical estimation, and it is almost certainly spurious. On

the other hand, an additional E_g frequency around 850 cm^{-1} should be expected. Similarly, an additional A_g frequency around 215 cm^{-1} and three additional ones at about 420 , 850 , and 920 cm^{-1} , respectively, should be expected to occur. The observed A_g frequency at about 350 cm^{-1} seems to be in particular disagreement with our calculations, much more than usual, and might also be spurious.

The agreement of the calculated infrared active modes with the measured spectra is also good, although a number of frequencies are missing, especially in the data measured on the single crystal, and at low frequencies. For instance, two A_u modes at 230 and 260 cm^{-1} , respectively, and an E_u mode around 230 cm^{-1} should exist according to our calculations; similarly, two E_u modes around 550 cm^{-1} and two more around 820 and 920 cm^{-1} , respectively, should also exist. On the other hand, the high E_u frequency at 1024 cm^{-1} and the one at 669 cm^{-1} , as well as the A_u frequencies at about 600 , 675 , and 720 cm^{-1} are irreconcilable with our model and very probably are not fundamentals: the last one was observed only by Gervais et al.,²⁴ and not by us. There is notable disagreement between the experimental values of the TO-LO splitting for some of the highest frequency modes, especially if the data presented by Gervais et al.²⁴ are considered, where in too many instances the reported LO values seem to be lower than their corresponding TO values; however, our experimental data do not show such inconsistencies, and furthermore, in general, our measured values for such splitting seem to agree much better with the corresponding theoretical estimates.

As a conclusion, the present work provides additional information about the optical vibrational spectra of phenakite, especially concerning the Raman-active modes; moreover, there are good reasons for believing that, besides giving the possibility of formulating reasonable estimates and interpretation of these vibrational spectra, our lattice-dynamical model applied to the whole crystal since the beginning can give important suggestions in selecting the fundamentals.

Acknowledgment. Financial contributions from CNR and MURST are gratefully acknowledged. The authors are also indebted to Messrs. Italo Campostrini and Luigi Saibene for valuable technical help.

References and Notes

- (1) Silvi, B.; D'Arco, Ph.; Saunders, V. R.; Dovesi, R. *Phys. Chem. Minerals* **1991**, *14*, 674.
- (2) Gramaccioli, C. M. *Int. Rev. Phys. Chem.* **1987**, *6* (4), 337.
- (3) Pilati, T.; Bianchi, R.; Gramaccioli, C. M. *Acta Crystallogr.* **1990**, *B46*, 301.
- (4) Pilati, T.; Demartin, F.; Cariati, F.; Bruni, S.; Gramaccioli, C. M. *Acta Crystallogr.* **1993**, *B49*, 216.
- (5) Pilati, T.; Demartin, F.; Gramaccioli, C. M. *Acta Crystallogr.* **1993**, *A49*, 473.
- (6) Pilati, T.; Demartin, F.; Gramaccioli, C. M. *Acta Crystallogr.* **1990**, *B50*, 544.
- (7) Pilati, T.; Demartin, F.; Gramaccioli, C. M. *Acta Crystallogr.* **1995**, *B51*, 721.
- (8) Pilati, T.; Demartin, F.; Gramaccioli, C. M. *Acta Crystallogr.* **1996**, *B52*, 239.
- (9) Pilati, T.; Demartin, F.; Gramaccioli, C. M. *Am. Mineral.* **1996**, *81*, 811.
- (10) Pilati, T.; Demartin, F.; Gramaccioli, C. M. *Acta Crystallogr.* **1996**, *B53*, 82.
- (11) Pilati, T.; Demartin, F.; Gramaccioli, C. M. *Am. Mineral.* **1997**, *82*, 1054-1062.
- (12) Pilati, T.; Demartin, F.; Gramaccioli, C. M. *Phys. Chem. Minerals* **1998**, *25*, 83-93.
- (13) Pilati, T.; Demartin, F.; Gramaccioli, C. M. *Acta Crystallogr.* in press.
- (14) Winkler, B.; Dove, M. T.; Leslie, M. *Am. Mineral.* **1991**, *76*, 313.

- (15) Patel, A.; Price, G. D.; Mendelssohn, M. J. *Phys. Chem. Minerals* **1991**, *17*, 690.
- (16) Adams, D. M.; Gardner, I. R. *J. Chem. Soc., Dalton Trans.* **1974**, 1502.
- (17) Kim, C. C.; Bell, M. I.; McKeown, D. A. *Physica* **1995**, *B205*, 193.
- (18) McKeown, D. A.; Bell, M. I. *Phys. Rev.* **1997**, *B56*, 3114.
- (19) Pilati, T.; Bianchi, R.; Gramaccioli, C. M. *Acta Crystallogr.* **1990**, *A46*, 309.
- (20) Pilati, T.; Bianchi, R.; Gramaccioli, C. M. *Acta Crystallogr.* **1990**, *A46*, 485.
- (21) Downs, R. T.; Gibbs, G. V. *Am. Mineral.* **1987**, *72*, 769.
- (22) London, R. *Adv. Phys.* **1964**, *13*, 423.
- (23) Hofmeister, A. M.; Hoering, T. C.; Virgo, D. *Phys. Chem. Minerals* **1987**, *14*, 205.
- (24) Gervais, F.; Piriou, B.; Cabannes, F. *Phys. Status Solidi B* **1973**, *55*, 143.
- (25) Dove, M. T. *Am. Mineral.* **1989**, *74*, 774.
- (26) Kim, C. C.; Bell, M. I.; McKeown, D. A. *Phys. Rev.* **1993**, *B47*, 7689.
- (27) Nye, J. F. *Physical Properties of Crystals*; Clarendon Press: Oxford, U.K., 1957.